

Experimental and modelling optimisation of sustainable techniques for the pre-treatment of the organic fraction municipal solid waste to improve anaerobic digestion

Original

Experimental and modelling optimisation of sustainable techniques for the pre-treatment of the organic fraction municipal solid waste to improve anaerobic digestion / Demichelis, F.; Deorsola, F. A.; Robotti, E.; Cravotto, G.; Marengo, E.; Tommasi, T.; Grillo, G.; Fino, D.. - In: JOURNAL OF CLEANER PRODUCTION. - ISSN 0959-6526. - 399:(2023). [10.1016/j.jclepro.2023.136594]

Availability:

This version is available at: 11583/2981606 since: 2023-09-05T08:13:03Z

Publisher:

ELSEVIER SCIENCE

Published

DOI:10.1016/j.jclepro.2023.136594

Terms of use:

This article is made available under terms and conditions as specified in the corresponding bibliographic description in the repository

Publisher copyright

(Article begins on next page)

1 Experimental and modelling optimisation of sustainable techniques for the
2 pre-treatment of the organic fraction municipal solid waste to improve
3 anaerobic digestion

4 Francesca Demichelis^{1*}, Fabio Alessandro Deorsola¹, Elisa Robotti^{2*}, Giancarlo Cravotto³, Emilio
5 Marengo², Tonia Tommasi¹, Giorgio Grillo³, Debora Fino¹.

6 ¹Department of Applied Science and Technology (DISAT), Politecnico di Torino, Corso Duca degli
7 Abruzzi 24, 10129 Torino, Italy

8 ²Department of Sciences and Technological Innovation, University of Piemonte Orientale, Viale
9 Michel 11, 15121 Alessandria, Italy

10 ³Department of Drug Science and Technology, University of Turin, via Pietro Giuria 9, 10125
11 Turin, Italy.

12 **Abstract**

13 The study investigated and compared the anaerobic digestion (AD) of real organic fraction municipal
14 solid waste (OFMSW) prior pre-treated with four types of pre-treatments: mechanical, thermal,
15 hydrodynamic-cavitation (HC), and ultrasound (US). The tested pre-treatments and AD
16 configurations were selected through Design of Experiments and then regression models were built
17 to find the most promising configurations in terms of biogas production and energetic sustainability
18 of the whole process. The novelty of the research is the simultaneously study of the working
19 conditions of the pre-treatments; and AD parameters like the two origins of the inoculum, its
20 incubation time, and the substrate: inoculum ratio (SI).

21 The results demonstrated that the best configurations of pre-treatments and AD were the ones
22 performed with thermal pre-treatment at 120 °C for 45 min (with inoculum incubation of 10 d at
23 substrate: inoculum (SI) ratio of 2:1) and HC at 55 °C (with inoculum incubation of 10 d at SI of 3:1).

24 The thermal, and to some extent the mechanical pre-treatment, evidenced as significant the interaction
25 between the pre-treatment time and the inoculum incubation time. AD of US-OFMSW achieved the
26 lowest performances since inhibition occurred, probably due to the lignocellulosic inhibitors release
27 after ultrasound pre-treatment.

28

29 **Keywords:** anaerobic digestion, pre-treatments, kinetic, energy sustainability, design of experiments,
30 surface response

31 **Abbreviation**

32 AD: anaerobic digestion

33 CAS: mesophilic digestate of cow-agriculture sludge

34 COD: Chemical Oxygen Demand

35 DoE: design of experiment

36 DR: disintegration rate

37 HC: hydrodynamic-cavitation
38 OFMSW: organic fraction municipal solid waste
39 TOC: Total Organic Carbon
40 TS: total solids
41 VS: volatile solids
42 WAS: mesophilic digestate of wastewater activated sludge.

43 **Highlights**

- 44 • Evaluation of technical and energetic sustainability of AD of pre-treated OFMSW.
- 45 • DoE provided the pre-treatment and AD configurations to test.
- 46 • Regression model detected the feasible and energetic sustainable AD processes.
- 47 • The interaction of pre-treatment and AD enhanced the methane production.
- 48 • Thermal and HC pre-treatments reached the highest energetic performances.

49

50 **Introduction**

51 Anaerobic digestion (AD) is a mature technology adopted to stabilise the organic matter and convert
52 it into biogas. Nowadays, the global warming change challenge is promoting the application of
53 renewable alternative sources of energy, and AD can enhance biogas production, which is a
54 renewable energy employed to produce heat-electricity and transport fuel. The above-mentioned
55 applications of biogas are not still widely implemented due to the higher costs of biogas production
56 rather than other renewable energy sources such as wind or photovoltaic. Nevertheless, biogas is an
57 energy which can be stored and used directly without conversions and is able to face the problem of
58 peak requirement and power failure (Scherzinger and Kaltschmitt, 2021). Due to these properties,
59 AD is a mature technology to face climate change and resource depletion and produce clean energy
60 (Hai et al., 2022) according to the Sustainable Development Goals.

61 The optimisation and improvement of AD consists in the study of the reactor design, the process
62 conditions (as temperature, pH, mixing, etc.), the feedstocks employed and its pre-treatment
63 (Kainthola et al., 2019). Based on the current scientific literature, pre-treatments may significantly
64 improve AD, considering both the efficiency of the pre-treatment and its effect on the overall AD.
65 The efficiency of the pre-treatment depends on the technique as well as on the type and composition
66 of substrate employed. The performance of AD depends on several factors: the kinetics and the
67 hydrolysis, the rate-limiting step, which depends on process conditions, the substrate composition,
68 and the biodegradability (Carmona-Cabello et al., 2018). In the literature, referring to AD, the term
69 biodegradability expresses the amount of material biologically convertible in methane. Complex
70 substrates can range from no biodegradable, as lignin, to complete biodegradable, as starch and sugar
71 (Cheah et al., 2019). Nevertheless, biodegradable compounds could have low degree of
72 bioavailability since part of the bio-matter can be incorporated into complex and barely biodegradable
73 lignocellulosic structures. In addition, substrates constituted by large particles will be slowly
74 degraded due to the actual limited surface area (Harun et al., 2019).

75 Currently, the pre-treatments are investigated for substrates as wastewaters from treatment plants,
76 crops-harvesting residues, wastes from the food industry, animal manure and organic fraction from
77 households. The Organic Fraction Municipal Solid Waste (OFMSW), considered in the present study
78 is a heterogeneous substrate, coming from the collection of municipal wastes including food industry
79 and households, with an average composition including easily biodegradable compounds (as 17.5 %
80 lipids, 17.7 % proteins, 17.1 % starch, 10.5 % free sugars), and harder biodegradable components (as
81 18.6 % cellulose, 9.7 % lignin and 8.6 % hemicellulose) (Pleissner and Peinemann, 2020).

82 In the last 40 years the most studied pre-treatments of organic wastes from the food industry and
83 households reported in the scientific literature available in Science Direct, concerning the laboratory
84 scale, are mechanical (35 %), thermal (26 %), ultrasonic (18 %), chemical (12 %) and microwaves (9
85 %).

86 Mechanical pre-treatments have been evaluated because the particle size significantly affects the
87 kinetics and stability of AD, determining the success or failure of the process.

88 Thermal pre-treatments have been performed at mild temperature because most part of OFMSW
89 consists of starch and hemicellulose, which can be hydrolysed at relative low temperatures (from 90
90 to 180 °C) with longer residence time (Li et al., 2017). Hydrothermal, steam explosion and vapour-
91 thermal are the most adopted thermal pre-treatments; among them, the vapour-thermal pre-treatment
92 requires a lower energy and a lower heating time compared to the hydrothermal and it could be done
93 with jacket reactors for a wide range of substrates, without water addition (Scherzinger and
94 Kaltschmitt, 2021).

95 Hydrodynamic cavitation (HC) prior to AD has provided a faster disintegration and the solubilization
96 of larger organic molecules, so that it could be easily digested by the microbial inoculum, promoting
97 a lower incubation time, higher degradation rates, and higher COD reduction with higher biogas
98 generation (Saxena et al., 2019).

99 According to (Demichelis et al., 2022), for AD in batch feeding mode, inoculum plays a key role and
100 the most important parameters for the inoculum are the incubation time (Zhang et al., 2019a), and
101 source, and the substrate: inoculum (SI) ratio (Zhang et al., 2019b).

102 For the best of author's knowledge, the available scientific studies about pre-treatments and AD
103 focused on them separately as in the studies from (Cesaro et al., 2014) and (Karthikeyan et al., 2018),
104 who reviewed the available pre-treatment methods for organic wastes before the AD process. Other
105 studies focused on: i) the evaluation of the pre-treatment performances through the disintegration
106 rate, as in (Demichelis et al., 2018); ii) on the effects of pre-treatments (use of acid or alkaline
107 reagents, and effect of temperature) on the AD of waste activated sludge from the perspectives of
108 organic matter composition, thermodynamics, and multi-omics, as in (Chen et al., 2022); iii) by
109 considering the improvement of AD after the pre-treatments, by an approach based on Anaerobic
110 Digestion Model 1 (ADM1), as in (Huang et al., 2021) and (Wang et al., 2020). All these studies
111 revealed that pre-treatment is a fundamental step with recalcitrant feedstocks to improve the methane
112 yield; but, they did not investigate the interaction between pre-treatments and AD, which can be
113 accomplished only if the conditions of both phases are changed contemporarily. The present study
114 evaluated the AD of real OFMSW after pre-treatment with four types of pre-treatments: mechanical,
115 thermal, HC, and US. The study concerned experimental tests and modelling. The experimentally
116 tested pre-treatments and AD configurations were selected through DoE, then the enhancement of
117 AD process (pre-treatment and AD) was evaluated in terms of biogas and methane productions, VS
118 removal, kinetic study, and ESI.

119 The novelty of the study was the optimization of AD considering the combined effect and the
120 interaction between pre-treatment and AD: this was possible by varying simultaneously the
121 conditions of the two phases according to DoE, instead of simply adopting these pre-treatments before
122 AD. The results of the experimentation, were used to build a regression model correlating the factors
123 involved in the study, their interactions, and their quadratic effects, to the production of biogas and
124 ESI, to obtain predictive models for the identification of the best running conditions for pre-treatment

125 and AD. In the results section, the best running condition will be detected for each type of pre-
126 treatment by separately considering the biogas, the kinetic and the ESI results. In the conclusion
127 section the best overall running conditions will be identified, among all the tested pre-treatments, by
128 combining the results obtained for biogas production, kinetics, and ESI.

129 These results are of fundamental importance since there is a lack of information to understand the
130 simultaneous effect of different pre-treatment techniques on AD performances, that should be
131 urgently studied to improve the whole AD process according to (Atelge et al., 2020) and (Abraham
132 et al., 2020).

133 **Material and methods**

134 **2.1 Substrate and inoculum characterisation**

135 AD of OFMSW, provided by San Carlo S.p.A (Fossano, Italy), was performed with two inocula: the
136 mesophilic digestate of wastewater activated sludge (WAS), according to (Kumar Biswal et al.,
137 2020), provided by SMAT (Torino, Italy), and the mesophilic digestate of cow-agriculture sludge
138 (CAS), based on (Gu et al., 2020), supplied by “Cascina La Speranza” (Fossano, Cuneo, Italy).

139 The OFMSW, WAS and CAS were characterised in Table 1. VS/TS and TOC contents of OFMSW
140 were higher than 90 % and 8,000 mg/kg, respectively; and this abundance of organic matter proved
141 the suitability of OFMSW to be employed as feedstock for AD (L.Zhang et al., 2019). OFMSW had
142 acid pH (5.6 ± 0.2), but the addition of WAS and CAS inocula increased the buffer capacity, since
143 their pH were 7.1 ± 0.1 (for WAS) and 7.7 ± 0.1 (for CAS). The physical-chemical properties of WAS
144 agreed with (Suksong et al., 2019) and the ones of CAS agreed with mixtures of inocula from dairy
145 manure and agricultural residues as reported in (Chen et al., 2008).

146 The C:N ratio of CAS was more suitable for AD than that of WAS, due to the higher carbon to
147 nitrogen balance. CAS (a mix of cow manure and agricultural residues) could improve AD for its
148 C:N ratio because the inhibition effect of nitrogen and ammonia from manure was limited by the
149 carbon deriving from agricultural residues.

150 Table 1: Physical and chemical properties of OFMSW and inocula.

	TS	VS	pH	C	H	N	S	C/N	TOC
	(%)	(%)	(-)	(%)	(%)	(%)	(%)	(-)	(g/kg)
OFMSW (mean)	19.32	96.76	5.31	48.42	6.76	2.97	0.20	16.3	24,995.82
OFMSW (dev.st)	0.61	0.53	0.22	0.51	0.70	0.32	0.12	1.4	114.92
WAS (mean)	5.09	70.7	7.12	35.42	3.04	4.51	0.01	7.92	9.52
WAS (dev.st)	0.11	1.0	0.11	0.51	0.02	0.11	0.01	0.14	0.12
CAS (mean)	5.82	70.3	7.74	40.62	3.09	7.92	0.03	5.12	12.04
CAS (dev.st)	0.12	1.0	0.12	0.61	0.07	0.11	0.01	0.12	0.24

151 2.2 Physical pre-treatments

152 In the present study the focus was on AD performed on pre-treated OFMSW. The DoE investigated
153 the pre-treatments and the AD, to evaluate, specifically for mechanical and thermal pre-treatments,
154 the interactions between these two steps (pre-treatment and AD).

155 The mechanical pre-treatment was performed with the mixer blender (Aigostar Archer 30RKN,
156 China) of 1.8 L, at three maximum speed values (15, 30, 45 and 60 min) (Gagić et al., 2018), requiring
157 0.023 kWh/L.

158 The thermal pre-treatment was performed in the heating bath (Corio C Julabo, Merck, Germany) at
159 three temperature values 60, 90 and 120 °C (Bruni et al., 2010) and for three time periods (15, 30 and
160 45 min), settled according to the mechanical pre-treatment. The energies to perform the pre-
161 treatments were 0.040 kWh/L for T = 60 °C, 0.048 kWh/L for T = 90 °C and 0.059 kWh/L for T =
162 120 °C.

163 Two hydrodynamic-cavitation (HC) pre-treatments were performed using a rotor/stator HC unit
164 (Rotocav[®], E-PIC srl – Mongrando, Italy) at two temperatures (25 and 55 °C) for 10 min (Bruni et
165 al., 2010). The two pre-treatments required 0.022 kWh/L and 0.073 kWh/L.

166 The ultrasound pre-treatment (US) was performed in a 3 L powerful multiprobe reactor (Weber
167 Ultrasonics AG, Karlsbad - Germany) for 30 min at 22 Hz and 200 W (Lauberte et al., 2021),
168 requiring 0.020 kWh/L.

169 2.2.1 Pre-treatment evaluation

170 The evaluation of each pre-treatment was performed through the Disintegration Rate (DR) (Eq.1 -2)
171 (Bougrier et al., 2005).

$$172 DR_{COD}(\%) = \frac{SCOD_1 - SCOD_0}{TCOD - SCOD_0} \cdot 100 \quad (1)$$

$$173 DR_N(\%) = \frac{SN_1 - SN_0}{TN - SN_0} \cdot 100 \quad (2)$$

174 where $SCOD_0$ and $SCOD_1$ are the Soluble Chemical Oxygen Demand (SCOD) before and after pre-
175 treatment, respectively; TCOD is the total COD; SN_0 and SN_1 are the soluble nitrogen before and
176 after pre-treatment, respectively, and TN is the total nitrogen.

177 Total and soluble COD and total nitrogen were detected through a COD LCI 400 and a LCK 338
178 (HACH LANGE GHB, Germany) and quantified by a spectrophotometer 5000 D, (HACH, Canada).

179 **2.3 Anaerobic digestion set up**

180 AD was performed on OFMSW in 1.0 L Pyrex glass bottles (Duran, Germany) with a working
181 volume of 80 %, at 37 °C, placed in a 55 L thermostatic water-bath (Julabo-Corio-C, Merck,
182 Germany), operating in batch mode with 6 % total solids (TS) of OFMSW. Each bioreactor was
183 manually shaken, and AD ended when biogas production was below 1%v/v of the total volume of
184 biogas produced up to that time (Angelidaki et al., 2009).

185 Each bioreactor was connected by 6 mm Teflon tubes (PTFE, Germany) to a gasholder, made by 2 L
186 Pyrex glass bottles (Duran, Germany). Biogas was analysed qualitatively by a biogas-analyser
187 (GA5000, GMBH, Germany) and quantitatively by water displacement.

188 AD on not pre-treated OFMSW was performed as control to detect increase or decrease of the
189 performances with respect to pre-treated OFMSW.

190 The WAS and CAS inocula, selected considering a previous study (Demichelis et al., 2022), were
191 separately cultivated under anaerobic conditions at 37°C in 2 L Pyrex glass bottles (Duran, Germany),
192 for three different periods (0, 5 and 10 d) and then inoculated in the pre-treated OFMSW considering
193 the Substrate: Inoculum (SI) ratio ranging from 1:2 to 2:1 for mechanical and thermal pre-treatment
194 and from 1:3 to 3:1 for HC and US, based on volatile solids (VS) (Demichelis et al., 2022). Since HC

195 and US pre-treatments were already optimised in (Lauberte et al., 2021), tests were performed on the
196 effect of the SI ratio.

197 **2.4 Analytical methods**

198 The OFMSW and the two inocula (WAS and CAS), were physically and chemically characterized.
199 TS and VS content were detected according to UNI EN 15216:2021 and elemental analysis (CHNSO)
200 was performed through an Elemental Macro Cube system (Vario, Germany).

201 The VS removed at the end of AD was evaluated through Eq. 3 according to (Li et al., 2018):

$$202 \text{ VS removed (\%)} = \frac{\text{VS input} - \text{VS output}}{\text{VS input} - (\text{VS input} \cdot \text{VS output})} \cdot 100 \quad (3)$$

203 where VS removed is the percentage of removed volatile solids, VS input and VS output are the
204 volatile solids concentrations in the feed substrate before and after AD.

205 The pH was measured according to DIN 38404 C5 methodology with a pH340 WTW pH-meter
206 (Mettler Toledo, Germany).

207 **2.5 Design of experiments**

208 The adopted Design of Experiment (DoE) identified the role played by the factors, their interactions,
209 and quadratic effects, and accomplished the optimization of the system with the final identification
210 of the best conditions for process running.

211 For mechanical and thermal pre-treatments, the DoE involved the simultaneous study of factors
212 related to pre-treatment and to AD to identify the effect eventually played by the interaction between
213 these two phases.

214 For HC and US pre-treatments, the DoE involved only the optimization of AD since the pre-
215 treatments were previously optimized (Calcio et al., 2018) (Lauberte et al., 2021).

216 Different DoEs were adopted to optimize the four pre-treatments since they differed from the number
217 of factors to be studied; moreover, some practical constraints needed to be taken into account: i) the
218 maximum number of experiments that could be run simultaneously, due to the number of available
219 AD reactors; ii) the necessity to simultaneously run all the experiments related to a single pre-
220 treatment to guarantee a lower experimental error; iii) the necessity to add some replications of the

221 experiments to evaluate the experimental error. See the supplementary material for the complete list
222 of experiments established by DoE and the types of models investigated.

223 For AD, three experimental factors were considered:

- 224 ● inoculum incubation (INOC), set at three levels: 0, 5 and 10 d (Demichelis et al., 2022).
- 225 ● SI, set at: i) three levels (1:2, 1:1 e 2:1) for mechanical and thermal pre-treatments, according
226 to the ones investigated in (Demichelis et al., 2022), and ii) at five levels (1:3, 1:2, 1:1, 2:1,
227 3:1) for HC and US according to (Liu et al., 2019) and (Kawai et al., 2014).
- 228 ● origin of inoculum (ORIG), set at two levels, namely WAS and CAS (Demichelis et al., 2022).

229 ORIG was a qualitative factor, hence the experiments identified by the DOEs were repeated for CAS
230 and WAS independently.

231 The DoE investigated the performances of the biodegradation of OFMSW; and specific biogas
232 production (NL/kg vs) and ESI (-) were selected as the experimental responses to be modelled. The
233 response surface methodology provided the best experimental conditions through a grid search
234 algorithm exploring the obtained models in the overall experimental domain (scaled in the range [0,1]
235 for each factor) with a step of 0.1 for each factor included in the model.

236 **2.5.2 DoE for mechanical and thermal pre-treatments**

237 For mechanical and thermal pre-treatments, the DOE included both the pre-treatment and the AD.
238 For the AD, INOC was studied at three levels (0, 5 and 10 d), SI at three levels (1:2, 1:1 and 2:1) and
239 ORIG at two qualitative levels (WAS and CAS) (Demichelis et al., 2022).

240 For the pre-treatments, the experimental factors were settled according to the study of DR_{COD} and
241 DR_N developed in the present study (section 3.2):

- 242 ● For the mechanical pre-treatment: the time of pre-treatment ~~was added~~ (PT) was studied at
243 three levels (15, 30 and 45 min)
- 244 ● For the thermal pre-treatment two factors were added: the temperature (TEMP) at three levels
245 (60, 90 and 120° C) and the time of pre-treatment (PT) at three levels (15, 30 and 45 min).

246 For the mechanical pre-treatment a central composite design was adopted with two replications of the
247 centre of the domain to evaluate the experimental error. The resulting 16 experiments are reported in
248 Table S1.

249 For the thermal pre-treatment, a fractional factorial design (FFD) 2^{4+1} was adopted, where the fourth
250 factor (SI) was confounded with the interaction between the first two (PT*TEMP), providing a total of
251 $2^3=8$ experiments. A star design was added, providing $2p+1 = 2*4+1=9$ experiments (p being the
252 number of factors), to evaluate the quadratic effects. Two more replications of the centre of the
253 domain were added to evaluate the experimental error, providing a total of 20 experiments, reported
254 in Table S2.

255 **2.5.3 DoE for hydrodynamic cavitation and ultrasound**

256 Since HC and US pre-treatments were previously optimised (Calcio et al., 2018) (Lauberte et al.,
257 2021), only AD was investigated considering the SI ratio at five levels (1:3, 1:2, 1:1, 2:1, 3:1)
258 according to (Liu et al., 2019) and (Kawai et al., 2014), while INOC was studied at three levels (0, 5
259 and 10 d). The DoE involved all the possible combinations of the levels for both factors, providing a
260 total of $5*3=15$ experiments with one more experiment consisting in a replication of the centre of the
261 domain to evaluate the experimental error. The resulting 16 experiments are reported in Table S3.
262 For HC, the DoE was repeated independently at 25 and 55 °C.

263 **2.6. Calculation of Regression Models**

264 For each DoE, regression models were assessed relating biogas production and ESI to the investigated
265 factors, their interactions, and their quadratic effects, independently for CAS and WAS origins. Only
266 statistically relevant (α -level < 0.05) coefficients, identified by ANOVA (Analysis Of Variance),
267 were included in the final models (Box, G., Hunter, S., 2005). See Supplementary Material for the
268 description of the coefficients included in each evaluated model.

269 **2.7 Kinetic study**

270 The kinetics of AD was studied to evaluate the disintegration rate (k_d) and the biogas volumetric rate.
271 The k_d was calculated by a first-order kinetic model Eq. (4):

272 $B(t) = B_{exp}(1 - e^{-k_d t})$ (4)

273 where $B(t)$ is the cumulative methane production at given time t (d), B_{exp} represents the ultimate
 274 methane potential yield (NL/kg vs) at the 5th day, k_d is the first-order disintegration rate (1/d) and t is
 275 the time of the process (1/d).

276 The biogas volumetric rate was calculated through Eq.5

277 $V \text{ biogas rate } \left(\frac{L}{L \cdot d} \right) = \frac{\text{Biogas (L)}}{\text{Volume of reactor (L)} \cdot \text{time (d)}}$ (5)

278 **2.9 Energy sustainable index**

279 The energetic sustainability of AD was measured with the energy sustainable index (ESI) calculated
 280 according to (Kovalovszki et al., 2020) and Eq. (6):

281 $ESI = \frac{Q_{pro}}{Q_s}$ (6)

282 where Q_{pro} was the energy produced from AD, considering that methane equals to 7.2 kWh/m³ (Rillo
 283 et al., 2020) and Q_s is the system thermal load measured in kWh (Eq. 7), and corresponded to the sum
 284 of the thermal power required for heating the substrate (Q_{sub}), the heat loss from the reactor walls
 285 (Q_{loss}), the heat loss through the tube (Q_p), according to (Mehr et al., 2017) and the energy consumed
 286 to perform the pre-treatments ($Q_{pre-treatment}$) with the specific consumption reported in sections 2.2
 287 for each type of pre-treatment.

288 $Q_s = Q_{sub} + Q_{loss} + Q_p + Q_{pre-treatment}$ (7)

289 **3.Results**

290 **3.1 Disintegration rate**

291 The study of the DR, calculated for COD and nitrogen (Figure 1), was performed to establish the
 292 suitable experimental domain for the factors included in the study of the four investigated pre-
 293 treatments, in terms of improvement of the available degradable matter (increase of the solubilisation
 294 of ready-digestible compounds of the OFMSW).

295 For the mechanical pre-treatment, the highest DR values were achieved after 45 min of pre-treatment,
296 whereas a further increase to 60 min did not show any statistically significant improvement of DR
297 and for the AD tests, a pre-treatment time of 60 min was not considered.

298 For the thermal pre-treatment, the highest DR values were achieved at the highest tested temperature
299 (120 °C) after 45 min of pre-treatment. By increasing the thermal pre-treatment time to 60 min, for
300 all the tested temperatures (60, 90 and 120 °C), no statistically significant differences were detected
301 ($\alpha - level = 0.05$), and a pre-treatment time of 60 min was not investigated in AD tests.

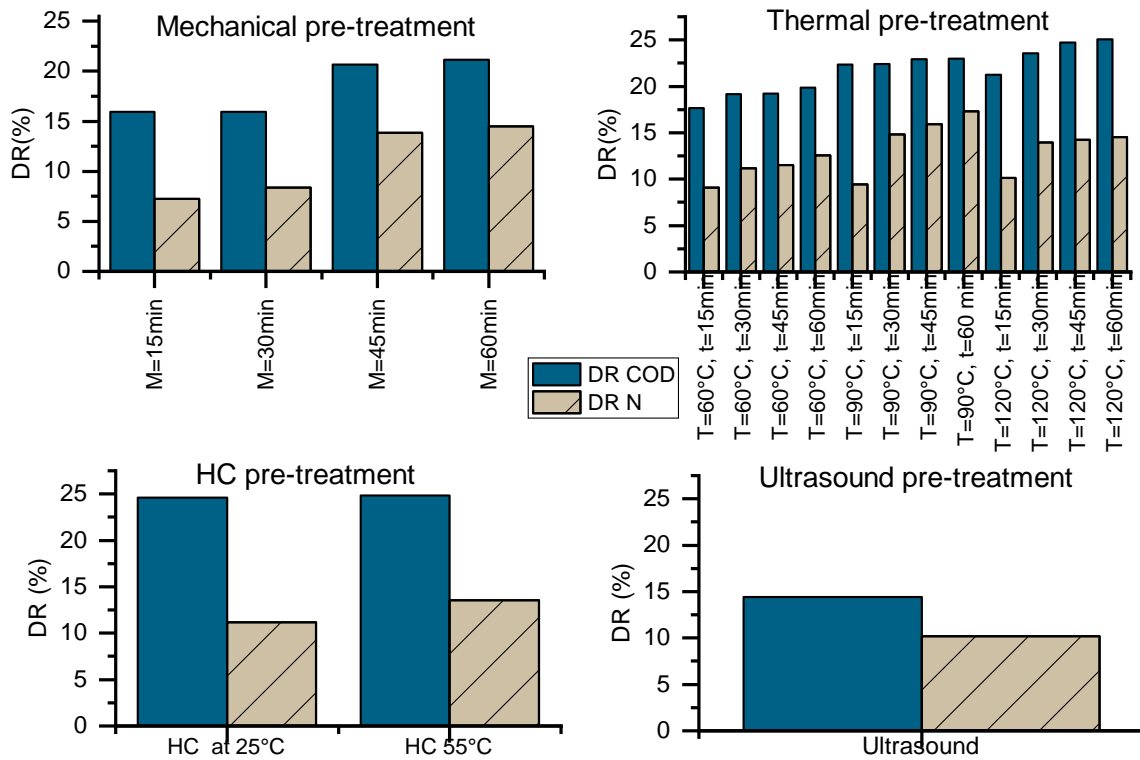
302 The results proved that, for thermal pre-treatments, the temperature played a more significant effect
303 than time, according to (Gagić et al., 2018).

304 No statistical differences were detected in DR calculated for COD and nitrogen, comparing HC at 25
305 and 55 °C; and these two configurations were tested.

306 Notwithstanding the worst results achieved by the US pre-treatment on DR for COD and nitrogen
307 (14.41 % and 10.21 %), compared to the other treatments, it was included in the experimentation
308 since it is considered as promising according to the literature (Lauberte et al., 2021).

309 Among the tested pre-treatments, those reaching the highest DR_{COD} , were: thermal pre-treatment at
310 120 °C for 45 min (27.85 %) and HC at 55 °C (27.92 %) and 25 °C (27.86 %), due to the synergic
311 effect of temperature and time, and for HC pre-treatments, the formation of extremely reactive
312 microenvironments generated inside the bubbles, characterized by intense pressure waves and
313 hydraulic jets, and responsible of a series of chemical and physical transformations in the OFMSW.

314 The DR indirectly describes the efficiency of degradation of complex organic substrates, but it only
315 quantifies the performances of the pre-treatment, neglecting its effect on AD.



316

317

Figure1: Disintegration rate (DR) of pre-treatments calculated for COD and nitrogen.

318

3.2 Biogas production

319

The AD performance was investigated through the evaluation of the productions of biogas and methane (Figure 2a), and the VS removal (Figure 2b), according to (Li et al., 2019), and through the response surfaces of the models calculated for biogas production (Figure 3).

321

322

3.2.1 Mechanical pre-treatment

323

In the case of AD of mechanically pre-treated OFMSW performed with WAS and CAS, the productions of biogas and CH₄ (Figure 2a: A1,A2) and the VS removal (Figure 2b: A1, A2) showed similar trends.

325

326

The surface responses (Figure 3A1 and A2) and the built models (Table S4) proved that the interaction between INOC and SI was relevant; and that the effect of INOC was similar for WAS and CAS, but, the models for biogas production with WAS showed higher R² value (R²= 0.9269, Table S4) than CAS (R²=0.8161), due to the absence of the SI parameter for the CAS origin ($\alpha < 0.05$). The biogas production (Figure 3A1 and A2) improves by increasing INOC at high SI (2:1). The quadratic effect

330

331 of INOC was also evident, while neither the linear nor the quadratic effect of the pre-treatment was
332 relevant.

333 The best experimental conditions, identified by the grid search algorithm (Table 9 2), were, for the
334 two inocula, at SI = 2:1, with INOC = 10 d and pre-treatment time of 15 min. For these configurations,
335 biogas and methane productions and VS removal were in the range: 695.46-699.17 NLbiogas/kg_{VS},
336 475.66-482.45 NL CH₄/kg_{VS} (Figure 2a: A1, A2), and 71.99- 73.52 % w/w for VS (Figure 2b: A1,
337 A2), which were higher than the ones reached in (Zhang and Banks, 2013) (VS removal in the range
338 57-64 % w/w for mesophilic AD of mechanically pre-treated OFMSW) due to the higher INOC (from
339 5 to 10 d).

340 The results proved that the particle size reduction did not notably increase the extent of degradation,
341 because the important aspect was the formation of a homogeneous substrate to feed AD without
342 impurities (Jain et al., 2015). The excess of smaller particles could lead to acid accumulation inside
343 the digester as proven by (Panigrahi et al., 2020); indeed, AD of mechanically shredded OFMSW
344 reached negligible different CH₄ content by reducing OFMSW particle size from 4 to 2 mm
345 (respectively 0.34 and 0.31 Nm³/kg_{VS}).

346 **3.2.2 Thermal pre-treatment**

347 For AD of thermally pre-treated OFMSW with WAS and CAS inocula, the biogas and CH₄
348 productions (Figure 2a: B1, B2) and VS removal (Figure 2b: B1, B2) showed similar trends.

349 The models for biogas production exhibited similar R² values for CAS (R²= 0.9630) and WAS (R²=
350 0.9644), and, for both inocula, PT showed a significant interaction with the INOC (Figure 3B1, Table
351 S5), while it was negligible as linear factor. This result was due to the higher buffering capacity of
352 the incubated inoculum, which produced the acclimatised micro-organisms able to biodegrade the
353 OFMSW (Zhang et al., 2019a).

354 Figures 3B1, B2, and B3 represent only the response surfaces for WAS (the factors not represented
355 are in turn fixed at the central value), since the two origins showed similar response surfaces. The

356 quadratic effect of INOC was evident, and changes in INOC correspond to the most significant
357 increases of the experimental response.

358 With the two inoculum origins, the configurations with pre-treatment at the highest temperature (120
359 °C) and the highest INOC (10 d) showed statistically negligible differences if pre-treatment was
360 performed for 15 or 45 min, because at the highest temperature, the pre-treatment time was negligible
361 due to the solubilisation and degradation effects played by the temperature (Li et al., 2017). This
362 result is in agreement with the literature: the increase of temperature promoted the feedstock
363 conversion degree, and the pre-treatment temperature affected AD performances more than pre-
364 treatment time according to (Gagić et al., 2018). Thermal pre-treatment is usually carried out at a
365 higher temperature (from 150 to 200 °C), but its main drawback is the high energy requirement, which
366 usually cannot be balanced by the high biogas production, leading to the consequential reduction of
367 the economic overall profitability of the process (Rajput et al., 2018). The optimal conditions
368 identified through the grid search algorithm (Table 2) were, for the two inocula, at SI= 2:1, INOC =
369 10 d, and pre-treatment at 120 °C for 15 min: the biogas production was predicted to be equal to 665
370 NLbiogas/kgvs in these conditions, which were not included in the DoE.

371 **3.2.3 HC pre-treatment**

372 The AD performances on HC-treated OFMSW at 25 (Figure 3: C1, C2) and 55 °C (Figure 3: D1, D2)
373 were similar.

374 The model for biogas with CAS reached $R^2= 0.9394$ at 25 °C and 0.9305 at 55 °C, higher than those
375 obtained with WAS ($R^2=0.8474$ at 25 and 55° C, Table S6). For CAS, the model contained all the
376 parameters, whereas, for WAS, the model excluded SI and the quadratic effect of INOC. For all the
377 models, all the parameters were statistically significant ($\alpha < 0.05$).

378 The biogas productions of HC at 25 and 55 °C with CAS (Fig.23: C2 and D2) provided comparable
379 results: a quadratic effect was evident for SI and INOC, proving their synergic effect in increasing
380 the biogas production. The best conditions identified by the grid search algorithm were at high levels

381 of INOC, equal to 8 d for HC at 25 °C (predicted biogas production = 700.62 NL/kg_{vs}) and 9.5 d for
382 HC at 55 °C (predicted biogas production = 798.07 NL/kg_{vs}), at SI = 3:1.

383 For HC at 25 and 55 °C with WAS (Fig.3 C1 and D1), the maximum biogas production occurred at
384 high INOC values (from 5 to 10 d) and medium-high value of SI (from 2:1 to 3:1), due to its evident
385 quadratic effect. The best conditions identified by the grid search algorithm (Table 2), for HC, at 25
386 and 55 °C, with WAS were: INOC = 10 d at SI = 2.74 (predicted biogas production = 670.44 NL/kg
387 vs. for HC at 25°C and 705.36 NL/kg vs for HC at 55°C).

388 The AD of HC-OFMSW at 55 °C achieved higher biogas and CH₄ productions (Figure 2a: C, D) than
389 HC at 25 °C, since during the collapse phase realised by HC, the highest temperature promoted the
390 formation of more reactive microenvironments which boosted the diffuse turbulence, the phase
391 changes, and the heat exchanges, occurring from macro to micro scales (Calcio et al., 2018).

392 **3.2.4 Ultrasound pre-treatment**

393 For US pre-treatment, the biogas and CH₄ productions and VS removal had similar trends for AD
394 performed with WAS and CAS inocula, but the AD performed with CAS inoculum reached higher
395 performances (Figure 2a: E; Figure 2b: E).

396 The model for biogas with CAS reached higher R² value (R²= 0.9286, Table S7) than WAS
397 (R²=0.8756), with a model containing INOC, the quadratic effect of SI and the interaction between
398 INOC and SI for both origins ($\alpha < 0.05$). By increasing INOC, the biogas production increased
399 independently of SI (Figure 3: E1, E2), whereas SI showed a significant quadratic effect at high INOC
400 values. These results proved the suitability of the incubated inoculum to treat higher OFMSW
401 amounts and to promote its degradation (Zhang et al., 2019a).

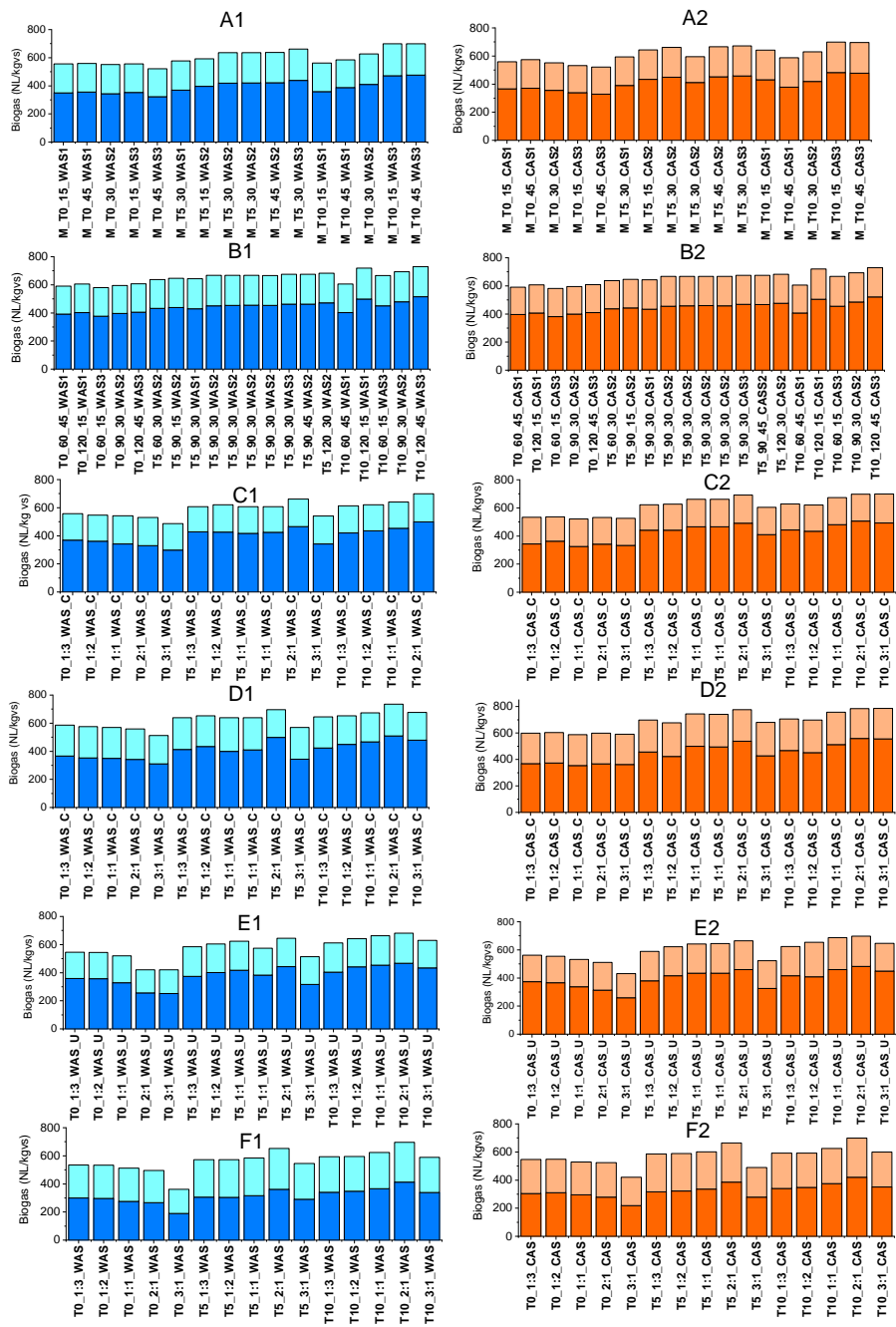
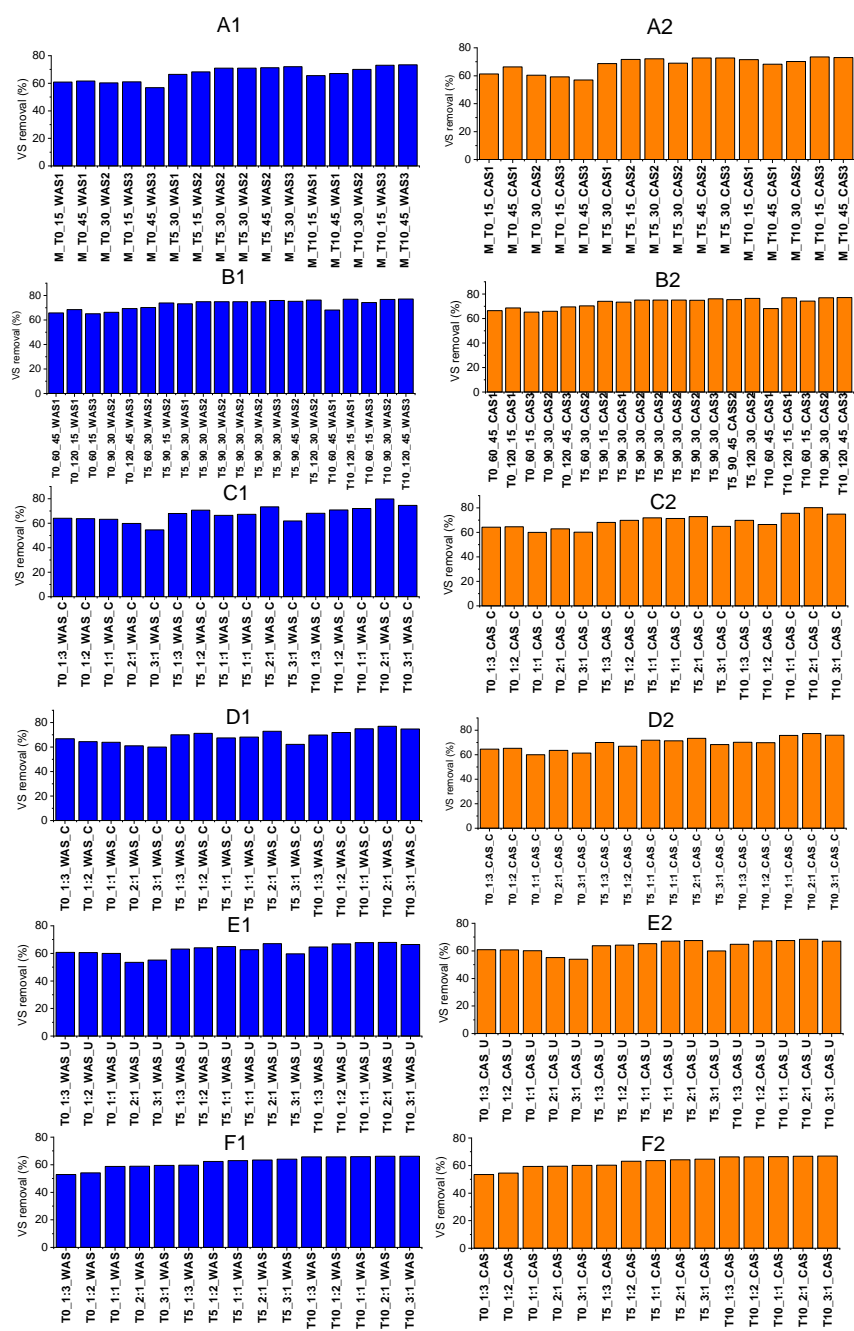
402 The optimal conditions identified by the grid search algorithm corresponded to INOC =10 d: at SI =
403 2.74 for WAS (predicted biogas production = 683.95 NL/kg_{vs}) and SI= 2.34 for CAS (predicted
404 biogas production = 703.63 NL/kg_{vs}) (Table 92). These results agreed with (Rasapoor et al., 2016)
405 where US was carried out on 6 % TS OFMSW for 30 min at 200 kHz.

406 Among the tested pre-treatments, US reached the lowest biogas and methane productions and VS
407 removals because probably the lipids accumulation negatively influenced AD since their degradation
408 was relatively slow and led to an accumulation of hydrophobic lipids which were adsorbed on the
409 microorganisms' surface (Hendriks and Zeeman, 2009) with the effect of limiting the mass transfer
410 process between microbial cells and dissolved organic matter (Scherzinger and Kaltschmitt, 2021).
411 The decrease of biodegradability after pre-treatment occurred for two main effects: formation of
412 refractory/toxic compounds (Carrère et al., 2009) and removal of organic material (Hendriks and
413 Zeeman, 2009). The US pre-treatment of the lignocellulosic fraction of OFMSW can release
414 hydroxymethylfurfural (HMF), furfural, and soluble phenols (Hendriks and Zeeman, 2009), or
415 produce melanoidins by uncompleted Maillard reactions (Pilli et al., 2011), which inhibit the AD.

416 **3.2.5 Comparison of the physical pre-treatments and no pre-treated OFMSW**

417 The performances of AD on physical pre-treated OFMSW were higher than those on untreated
418 OFMSW tested in (Demichelis et al., 2022) in 0.5 L bioreactors and re-tested in the present
419 manuscript in 2 L bioreactors to evaluate the scale effect (Figure S1).

420 The biogas production of mechanically pre-treated OFMSW was higher than untreated OFMSW, in
421 the ranges 3.0 and 7.3 % in agreement with (Coarita et al., 2020), 4.6- and 9.8 % for mild-thermal
422 pre-treatments in agreement with (Chen et al., 2020), 7.8 and 11.8 % with HC according to (Saxena
423 et al., 2019), 2.5- and 4.7 % with US as proved by (Rasapoor et al., 2016), since pre-treatments
424 increase the exposure of the biodegradable matter to microorganisms and vary the composition of
425 hardly degradable matter (Zhen et al., 2017).

a**b**

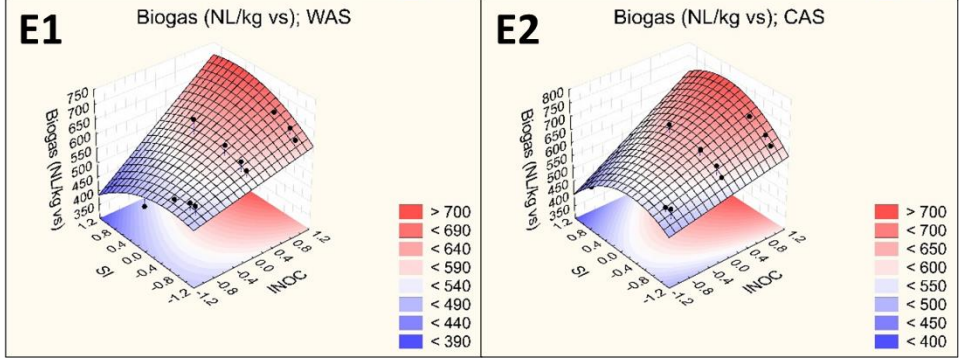
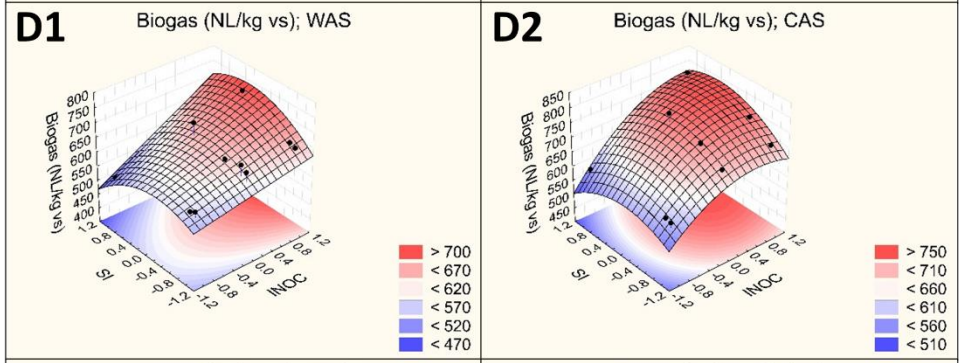
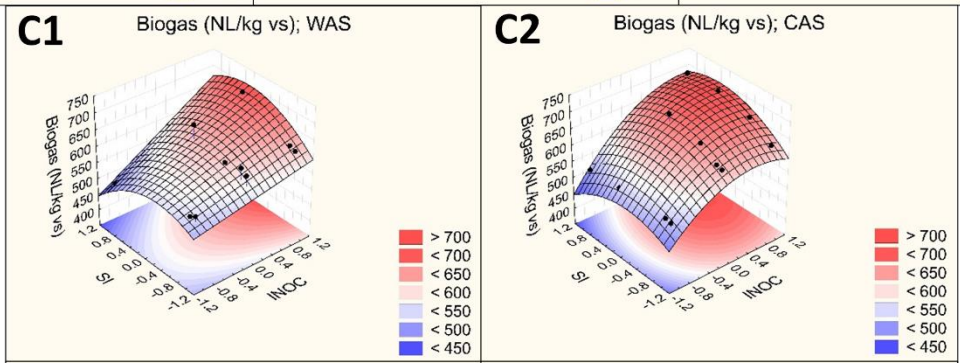
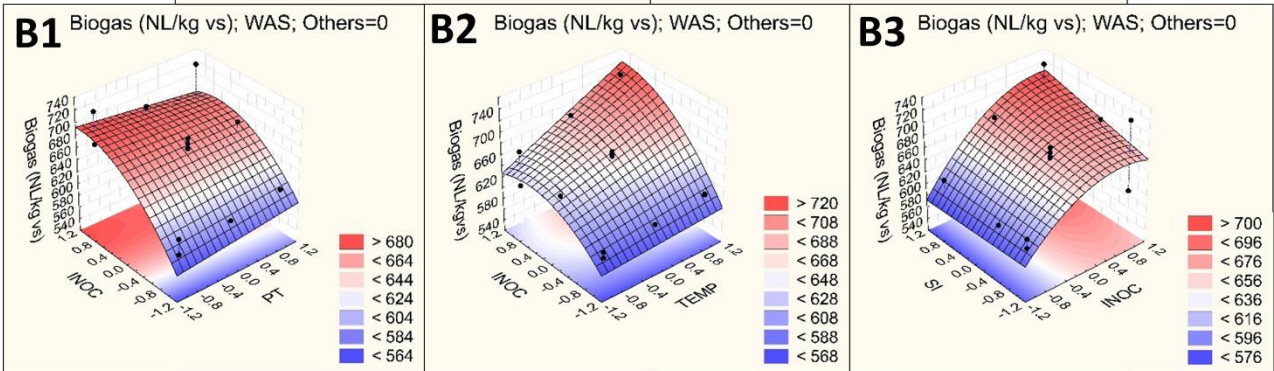
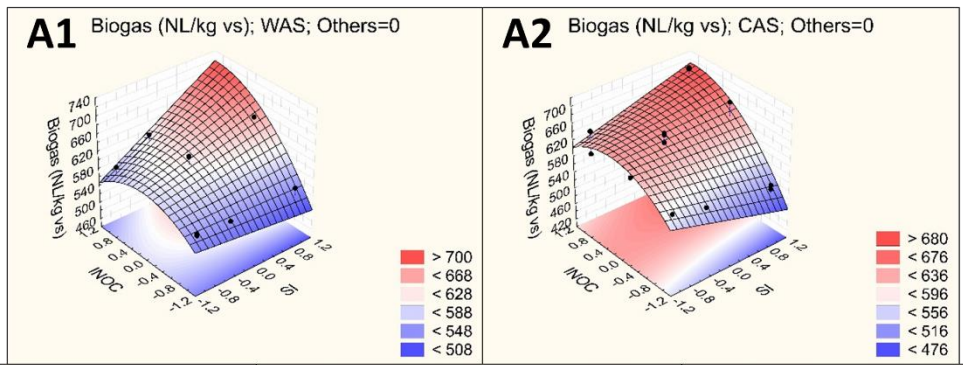
427

428 Figure 2a: Biogas production of AD on pre-treated and not pre-treated OFMSW: mechanical (A), thermal (B), hydrodynamic cavitation (HC) at
429 25°C (C), (HC) at 55 °C (D), ultrasound (E), no pre-treatment (F). On the left, AD configurations carried out with inoculum WAS are reported (dark
430 blue is methane, light blue is carbon dioxide), while those carried out with the CAS origin are reported on the right (dark orange is methane, light
431 orange is carbon dioxide).

432 Figure 2b: Volatile solids removal of AD performed on pre-treated and not pre-treated OFMSW: mechanical (A), thermal (B), HC at 25 °C (C), HC
433 at 55 °C (D), ultrasound (E), no pre-treatment (F). On the left, AD configurations carried out with inoculum WAS are reported (blue), while those
434 carried out with the CAS origin are reported on the right (orange).

435

436



439 Figure 3: Response surfaces of biogas production for the pre-treatments: mechanical (A1, WAS; A2,
440 CAS), thermal (B1, B2, B3, WAS). HC at 25°C (C1, WAS; C2, CAS), HC at 55°C (D1, WAS; D2,
441 CAS) and ultrasound (E1 for WAS; E2 for CAS). For thermal pre-treatment only the response
442 surfaces for WAS are depicted since the models for WAS and CAS are almost identical.

443 3.3 Kinetic study

444 The kinetic study proved the importance of the incubation time and of the origin of the inoculum
445 (Figure S1).

446 AD performed with INOC equal to 5 and 10 d promoted hydrolysis, acidogenesis, acetogenesis and
447 methanogenesis without inhibition, achieving the faster k_d and volumetric biogas rates.

448 The origin of the inoculum influenced the k_d , and CAS inoculum exhibited a faster degradation rate
449 than WAS, in agreement with (Kumar Biswal et al., 2020): because the proper C:N ratio of CAS
450 supported a correct development of the AD process (Calcio et al., 2018), and the incubation of the
451 inoculum provided acclimatised micro-organisms able to biodegrade the OFMSW (Zhang et al.,
452 2019a).

453 In all the tested pre-treatments, the values of k_d and biogas volumetric rate were linearly correlated.

454 In AD of mechanically pre-treated OFMSW, the highest volumetric biogas rate and k_d were achieved,
455 for the two inocula, by increasing INOC (5 and 10 d) and SI, without a significant effect of the
456 extension of the PT ($k_d = 0.33$ and 0.50 1/d), as proved by (Gagić et al., 2018). The study of (Motte et
457 al., 2015) stated that the fine milling of organic waste may simultaneously increase the AD kinetic
458 and failure (Victorin et al., 2020), whereas in the present study these risks were limited by the
459 presence of the incubated inoculum.

460 For AD of thermally pre-treated OFMSW, the highest volumetric biogas rate and k_d were achieved
461 by AD performed with INOC = 10 d, at SI = 2:1 and pre-treatment at 120 °C for 45 min: 3.31 with
462 WAS and 3.33 NL/kgvs·d with CAS (L. Zhang et al., 2019), and k_d equal to 0.51 and 0.53 1/d with
463 WAS and CAS respectively (Zhang et al., 2019b). These results proved that kinetic values increased
464 by increasing INOC (from 0 to 10 d) and pre-treatment temperature (Li et al., 2017), because the
465 incubation promoted the formation of acclimatised micro-organisms, while the temperature boosted
466 the solubilisation of the OFMSW improving its bio-degradation.

467 AD performed on HC-OFMSW at 25 and 55 °C with the two inocula, showed the same kinetic
468 configuration trends: the volumetric biogas rate and k_d increased by increasing the INOC (from 0 to

469 10 d and the HC temperature, due to the simultaneously effect of the inoculum incubation and the
470 higher capacity of extraction of bioactive compounds characteristic of HC performed at higher
471 temperature (Calcio et al., 2018).

472 AD of US pre-treated OFMSW reached the highest k_d and volumetric biogas rates with the highest
473 INOC = 10 d, notwithstanding the value of SI, for the two inocula.

474 For AD performed with incubated inocula, the k_d and volumetric biogas rates increased by increasing
475 the SI ratio, because the inoculum with acclimatised micro-organisms could be employed ~~in~~ with a
476 lower amount than a non-incubated inoculum (Zhang et al., 2019a).

477 The k_d of the four types of pre-treatments varied between 0.1 and 0.58 1/d , ranging from the lowest
478 to the highest specific biogas production, according to the optimal range of 0.134-0.56 1/d stated by
479 (Li et al., 2018). The k_d of carbohydrates ranged from 0.5 to 2.0 1/d, proteins varied between 0.25-
480 0.8 1/d and lipids ranged between 0.1 and 0.7 1/d , (Victorin et al., 2020). In the present study,
481 mechanical, thermal and US pre-treatments could promote the release of carbohydrate compounds,
482 whereas HC pre-treatment, a mix of carbohydrates and lipids.

483 The inocula incubation provided the optimal consortium of anaerobic microbes able to prevent
484 inhibition, due to the higher SI ratio (from 3:1 to 2:1) (Browne and Murphy, 2013), whereas the non-
485 incubated inocula negatively affected the lag phase (λ) and the maximum specific biogas production
486 (Dasgupta and Chandel, 2019).

487 Among the tested AD configurations, AD of HC-OFMSW reached the highest k_d , since HC is a
488 promising strategy to overcome the non-degradability of the recalcitrant components in AD (Naran
489 et al., 2016) (Saxena et al., 2019).

490

491 3.4 Energy sustainable index

492 3.4.1 Mechanical pre-treatment

493 The ESI major than 1 for AD performed on mechanically pre-treated OFMSW was reached by the
494 same ~~four~~ configurations with WAS and CAS, (Figure 4A1-A2, and Figure S2 and Table S4) but
495 different models were obtained for AD performed with CAS and WAS-(Table S4). The model for
496 WAS reached a lower R^2 (equal to 0.8963) and contained only INOC, while the model for CAS
497 contained INOC, PT and two interactions (SI * PT and SI * INOC), proving the relevant interaction
498 between the pre-treatment phase and the AD ($R^2 = 0.9369$).

499 In the case of WAS, no surface responses are provided since the model was simple and the best
500 conditions were obtained with high values of INOC (10 d) notwithstanding the values applied for PT
501 and SI; these two factors can be therefore kept at the most convenient value equal to PT =15 min at
502 SI= 2:1.

503 In the case of the CAS origin, looking at the ~~For the~~ surface responses , ~~for CAS~~ (Figure 34: A1, A2),
504 considering INOC*SI, the ESI increased by increasing INOC at high and low SI, since INOC (Table
505 S4) played the most significant role (Zhang et al., 2019a).

506 The best configuration stated by the grid search algorithm (Table 2) was, for the two inoculum origins,
507 PT=15 min, SI =2:1 and INOC =10 d, with a calculated response of 1.17 and 1.01 for CAS and WAS
508 (close to the experimental ones, 1.14 and 1.04).

509 3.4.2 Thermal pre-treatment

510 The ESI of AD on thermally pre-treated OFMSW reached the same trends with WAS and CAS
511 (Figure S2, 4B).

512 For thermal pre-treatment, the models with CAS and WAS reached high R^2 values ($R^2= 0.9882$ for
513 WAS and $R^2 = 0.9878$ for CAS, Table 6-S5), and contained the same parameters ($\alpha < 0.05$). The two
514 models were similar (Table S5), therefore, the response surfaces for the four significant interactions
515 were reported just for WAS (Figure 4: B1-B4). Considering the interactions, the trend of TEMP*PT
516 (Figure 4 B1) and TEMP*SI (Figure 4 B3) was similar one to each other and the same can be observed

517 for INOC*TEMP (Figure 4 B2) and INOC*SI (Figure 4 B4). Increasing TEMP, the ESI increased at
518 low PT values, according to (Rittmann et al., 2018), while an increase of PT increased ESI at low
519 TEMP values, without producing relevant effects at high TEMP values, in agreement with (Menardo
520 et al., 2015).

521 This result proved that the pre-treatment temperature was more effective than time since the
522 temperature boosted the solubilisation of the OFMSW reducing the ammonia concentration as the
523 result of caramelization or Maillard reactions occurring at temperature above 90 °C, preserving the
524 AD process.

525 The best configurations identified by the grid search algorithm for thermal pre-treatment (Table 2)
526 were AD with INOC=10 d at SI = 2:1, TEMP = 120°C and PT = 45 min for CAS (predicted ESI =
527 1.20), followed by AD with INOC = 10 d and SI = 1.74, TEMP =120 °C and PT = 45 min for WAS
528 (predicted ESI = 2.13).

529 **3.4.3 HC pre-treatment**

530 For HC at 25 °C, the models with the two inoculum origins reached high R^2 values ($R^2= 0.9635$ for
531 WAS and $R^2 = 0.9390$ for CAS, Table 2), whereas for HC at 55 °C, the model with CAS reached a
532 R^2 value higher than WAS ($R^2= 0.9455$ for CAS, $R^2 = 0.8842$ for WAS, Table 2).

533 The best conditions of ESI (Table 2, Figure 4: C1, C2, D1, D2) were: INOC = 10 d and SI values
534 ranging from 3:1 (WAS) to 2.87 (CAS) for HC at 25 °C and from 2.6 (WAS) and 2.74 (CAS) for HC
535 at 55 °C. The predicted ESI values ranged between 1.07 and 1.12. These results proved the importance
536 of temperature on the HC performance (Calcio et al., 2018).

537 The energy cost to carry out HC was covered by the biogas surplus produced by AD of HC-OFMSW,
538 assessing HC as an effective pre-treatment (Saxena et al., 2019). The HC had a positive ESI due to
539 lower plant and operating costs, higher process yields and energy savings due to shorter process times
540 (Calcio et al., 2018).

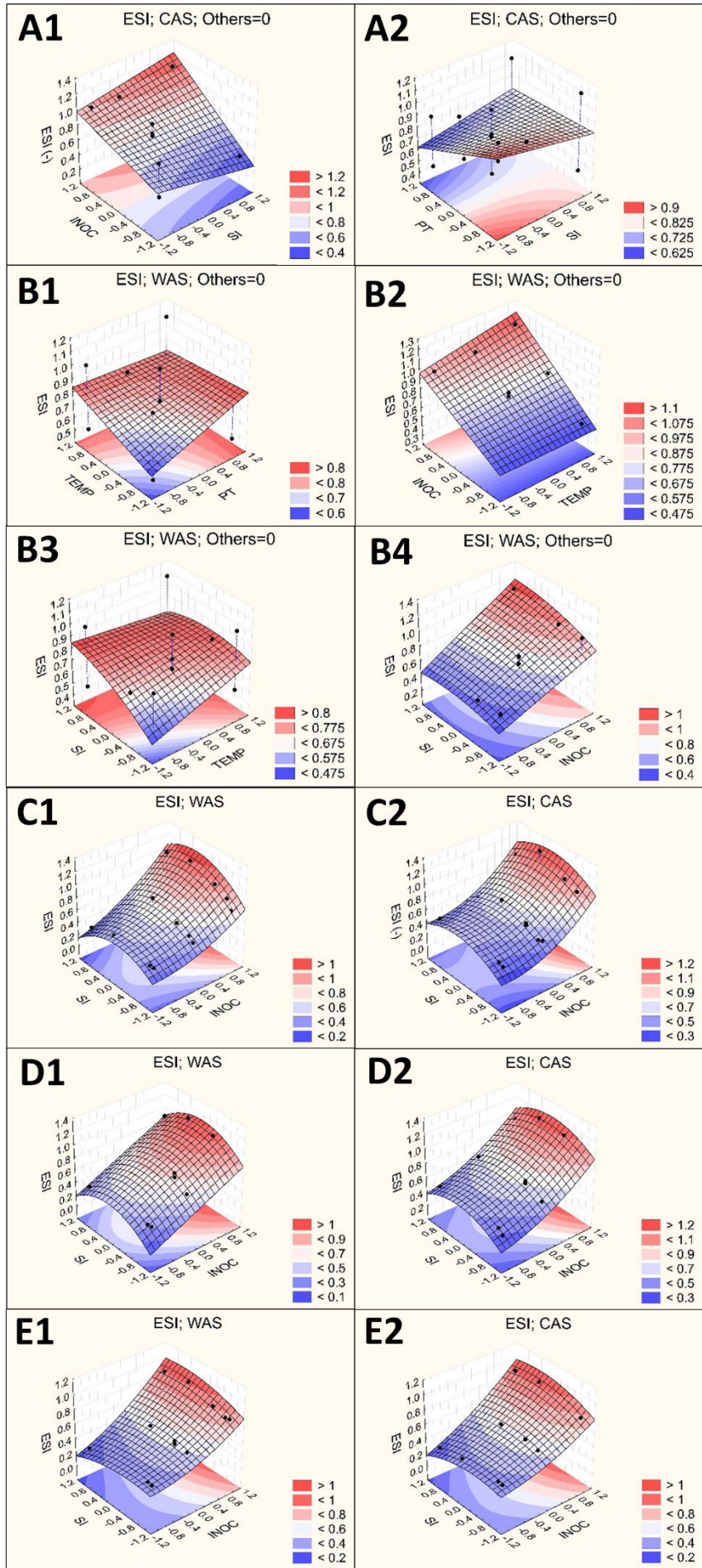
541 **3.4.4 Ultrasound pre-treatment**

542 All tested configurations for AD carried out on ultrasound pre-treated OFMSW, with CAS and WAS,
543 were energetically unsustainable (Figure S2E).

544 The model with WAS and CAS contained all the parameters ($R^2= 0.9832$ for WAS, $R^2=0.9775$ for
545 CAS, Table S7). The response surfaces (Figure 4: E1, E2) with WAS and CAS, proved that the
546 increase of INOC increased ESI notwithstanding SI values, whereas ESI increased and reached
547 almost a plateau by increasing SI at high INOC.

548 The best conditions identified by the grid search algorithm (Table 2) corresponded to INOC =10 d
549 and SI =3:1 for both origins, but the calculated responses with these conditions reached $ESI < 1$. The
550 energetic unsustainability of AD performed on US pre-treated OFMSW was due to the high energy
551 required to carry out the pre-treatments and lower CH_4 produced during AD (59.80 and 68.90 %v/v
552 with WAS and 60.34 and 69.52 %v/v with CAS) compared to the other pre-treatments.

553



555 **Figure 4:** Response surfaces of ESI for the four physical pre-treatments: mechanical (A1, A2),
 556 thermal (B1, B2, B3, B4), HC at 25°C (C1, C2), HC at 55°C (D1, D2) and ultrasound (E1, E2). For
 557 the mechanical and thermal pre-treatments only the response surfaces for WAS are reported since the
 558 models for WAS and CAS are almost identical.

559
 560 Table 2: Response prediction of AD of pre-treated OFMSW (/) is reported when the parameter was
 561 not included in the optimization; - is reported when the parameter can be kept at any level).

562

		Best conditions ranged between -1 and +1					Best conditions reported in the original measure units				
		PT	TEMP	INOC	SI	Y best	PT (min)	TEMP (°C)	INOC (d)	SI	
Mechanical	Biogas	WAS	-	/	1	1	703.00	-	/	10	2:1
		CAS	-	/	1	1	684.70	-	/	10	2:1
	ESI	WAS	-	/	1	-	1.01	-	/	10	-
		CAS	-1	/	1	1	1.17	15	/	10	2:1
Thermal	Biogas	WAS	-1	1	1	1	752.70	15	120	10	2:1
		CAS	-1	1	1	1	753.20	15	120	10	2:1
	ESI	WAS	1	1	1	0.65	2.13	45	120	10	1.74:1
		CAS	1	-1	1	1	1.20	45	60	10	2:1
HC Cavitation 25°C	Biogas	WAS	/	/	1	0.8	670.44	/	/	10	2.74:1
		CAS	/	/	0.8	1	700.62	/	/	8	3:1
	ESI	WAS	/	/	1	1	1.09	/	/	10	3:1
		CAS	/	/	1	0.9	1.12	/	/	10	2.87:1
HC Cavitation 55°C	Biogas	WAS	/	/	1	0.8	705.36	/	/	10	2.74:1
		CAS	/	/	0.9	1	798.07	/	/	9.5	3:1
	ESI	WAS	/	/	1	0.7	1.07	/	/	10	2.60:1
		CAS	/	/	1	0.8	1.12	/	/	10	2.74:1
Ultrasound	Biogas	WAS	/	/	1	0.8	683.95	/	/	10	2.74:1
		CAS	/	/	1	0.5	703.63	/	/	10	2.34:1
	ESI	WAS	/	/	1	1	0.90	/	/	10	3:1
		CAS	/	/	1	1	0.92	/	/	10	3:1

563

564 4. Conclusions

565 This study evaluated the AD of real OFMSW prior pre-treated with four types of pre-treatments:
566 mechanical, thermal, HC, and US, to optimise the whole process. The tested pre-treatments and AD
567 configurations were selected through DoE, considering the interaction between the pre-treatment and
568 the AD phases. The experiments of each DoE were evaluated by measuring the biogas production,
569 the VS removal, and the ESI. The results were used to build regression models correlating the
570 responses to the factors involved in the study, their interactions, and their quadratic effects.
571 The best configurations of pre-treatments and AD were the ones performed with thermal pre-
572 treatment at 120° C for 45 min and inoculum incubation of 10 d at SI equal to 2:1, due to the thermal
573 solubilisation effect, and HC at 55 °C and inoculum incubation of 10 d at SI equal to 3:1, for the
574 combined heat-bubbling effect, which enhanced the availability of the digestible fraction of OFMSW.
575 Pre-treatment time was significant only in the case of thermal pre-treatment and it showed a
576 significant interaction with the inoculum incubation time.
577 The AD of US-OFMSW achieved the lowest performances since inhibition occurred. In the future
578 the combined environmental and economic assessments of the four pre-treatments and AD will be
579 investigated.

580 **Statements and Declarations**

581 **Funding**

582 The authors gratefully acknowledge financial support from Region Piemonte (Italy), POR FESR
583 2014/2020, Project BIOENPRO4TO.

584 **Competing interests**

585 The authors declare no competing interests.

586 **Author's contributions**

587 Authors 'contributions are detailed in the following. F. Demichelis carried out the conceptualization
588 and experimental tests and wrote part of the paper. F.A. Deorsola contributed to realise the
589 methodology and wrote and reviewed the paper, T. Tommasi supported the structure of the study. G.
590 Cravotto optimised the hydrodynamic-cavitation and ultrasound pre-treatment tests and contributed

591 to write part of the paper; G.Grillo performed hydrodynamic-cavitation and ultrasound pre-treatment
592 tests; E. Robotti coordinated and realised the modelling study and contribute to write and review the
593 manuscript. E. Marengo contributed to modelling analysis and D. Fino realised the conceptualization
594 to supervision of the study.

595 **Data availability**

596 Data are complete reported in the manuscript and in the supplementary material.

597 **Acknowledgements**

598 The authors are grateful to Mr. Daniele Crudo (E-PIC srl - Mongrando (BI), Italy) for his valuable
599 technical assistance.

600

601 **References**

- 602 Abraham, A., Mathew, A.K., Park, H., Choi, O., Sindhu, R., 2020. Pretreatment strategies for
603 enhanced biogas production from lignocellulosic biomass. *Bioresour. Technol.* 301, 122725.
604 <https://doi.org/10.1016/j.biortech.2019.122725>
- 605 Angelidaki, I., Alves, M., Bolzonella, D., Borzacconi, L., Campos, J.L., Guwy, A.J., Kalyuzhnyi,
606 S., Jenicek, P., Lier, J.B. Van, 2009. Defining the biomethane potential (BMP) of solid
607 organic wastes and energy crops : a proposed protocol for batch assays. *Water Sci. Technol*
608 927–934. <https://doi.org/10.2166/wst.2009.040>
- 609 Atelge, M. R., Atabani, A.E., Banu, J.R., Krisa, D., Kaya, M., Eskicioglu, C., Kumar, G., Lee, C.,
610 Yildiz, Y., Unalan, S., Mohanasundaram, R., Duman, F., 2020. A critical review of
611 pretreatment technologies to enhance anaerobic digestion and energy recovery. *Fuel* 270,
612 117494. <https://doi.org/10.1016/j.fuel.2020.117494>
- 613 Bougrier, C., Carrère, H., Delgenès, J.P., 2005. Solubilisation of waste-activated sludge by
614 ultrasonic treatment. *Chem. Eng. J.* 106, 163–169. <https://doi.org/10.1016/j.cej.2004.11.013>
- 615 Box, G., Hunter, S., H., 2005. *Statistics for Experimenters.*, Second Edi. ed. Wiley., New Jersey,
616 USA
- 617 Browne, J.D., Murphy, J.D., 2013. Assessment of the resource associated with biomethane from
618 food waste. *Appl. Energy* 104, 170–177. <https://doi.org/10.1016/j.apenergy.2012.11.017>
- 619 Bruni, E., Jensen, A.P., Angelidaki, I., 2010. Steam treatment of digested biofibers for increasing
620 biogas production. *Bioresour. Technol.* 101, 7668–7671.
621 <https://doi.org/10.1016/j.biortech.2010.04.064>
- 622 Calcio, E., Tabasso, S., Grillo, G., Cravotto, G., Dreyer, T., Schories, G., Altenberg, S., Jashina, L.,
623 Telysheva, G., 2018. Comptes Rendus Chimie Wheat straw lignin extraction with bio-based
624 solvents using enabling technologies. *Comptes rendus - Chim.* 21, 563–571.
625 <https://doi.org/10.1016/j.crci.2018.01.010>
- 626 Carmona-Cabello, M., Garcia, I.L., Leiva-Candia, D., Dorado, M.P., 2018. Valorization of food

627 waste based on its composition through the concept of biorefinery. *Curr. Opin. Green Sustain.*
628 *Chem.* 14, 67–79. <https://doi.org/10.1016/j.cogsc.2018.06.011>

629 Carrère, H., Sialve, B., Bernet, N., 2009. Improving pig manure conversion into biogas by thermal
630 and thermo-chemical pretreatments. *Bioresour. Technol.* 100, 3690–3694.
631 <https://doi.org/10.1016/j.biortech.2009.01.015>

632 Cesaro, A., Velten, S., Belgiorno, V., Kuchta, K., 2014. Enhanced anaerobic digestion by ultrasonic
633 pretreatment of organic residues for energy production. *J. Clean. Prod.* 74, 119–124.
634 <https://doi.org/10.1016/j.jclepro.2014.03.030>

635 Cheah, Y.K., Vidal-Antich, C., Dosta, J., Mata-Álvarez, J., 2019. Volatile fatty acid production
636 from mesophilic acidogenic fermentation of organic fraction of municipal solid waste and food
637 waste under acidic and alkaline pH. *Environ. Sci. Pollut. Res.* 26, 35509–35522.
638 <https://doi.org/10.1007/s11356-019-05394-6>

639 Chen, H., Yi, H., Li, H., Guo, X., Xiao, B., 2020. Effects of thermal and thermal-alkaline
640 pretreatments on continuous anaerobic sludge digestion: Performance, energy balance and,
641 enhancement mechanism. *Renew. Energy* 147, 2409–2416.
642 <https://doi.org/10.1016/j.renene.2019.10.051>

643 Chen, Y., Cheng, J.J., Creamer, K.S., 2008. Inhibition of anaerobic digestion process : A review.
644 *Bioresour. Technol.* 99, 4044–4064. <https://doi.org/10.1016/j.biortech.2007.01.057>

645 Chen, Y., Ping, Q., Li, D., Dai, X., Li, Y., 2022. Comprehensive insights into the impact of
646 pretreatment on anaerobic digestion of waste active sludge from perspectives of organic matter
647 composition, thermodynamics, and multi-omics. *Water Res.* 226, 119240.
648 <https://doi.org/10.1016/j.watres.2022.119240>

649 Coarita Fernandez, H., Teixeira Franco, R., Bayard, R., Buffiere, P., 2020. Mechanical Pre-
650 treatments Evaluation of Cattle Manure Before Anaerobic Digestion. *Waste Biomass*
651 *Valorization.* <https://doi.org/10.1007/s12649-020-01022-4>

652 Dasgupta, A., Chandel, M.K., 2019. Enhancement of biogas production from organic fraction of

653 municipal solid waste using hydrothermal pretreatment. *Bioresour. Technol. Reports* 7,
654 100281. <https://doi.org/10.1016/j.biteb.2019.100281>

655 Demichelis, F., Fiore, S., Onofrio, M., 2018. Pre-treatments aimed at increasing the
656 biodegradability of cosmetic industrial waste. *Process Saf. Environ. Prot.* 118.
657 <https://doi.org/10.1016/j.psep.2018.07.001>

658 Demichelis, F., Tommasi, T., Deorsola, F.A., Marchisio, D., Fino, D., 2022. Effect of inoculum
659 origin and substrate-inoculum ratio to enhance the anaerobic digestion of organic fraction
660 municipal solid waste (OFMSW). *J. Clean. Prod.* 351, 131539.
661 <https://doi.org/10.1016/j.jclepro.2022.131539>

662 Gagić, T., Perva-Uzunalić, A., Knez, Ž., Škerget, M., 2018. Hydrothermal Degradation of Cellulose
663 at Temperature from 200 to 300 °c. *Ind. Eng. Chem. Res.* 57, 6576–6584.
664 <https://doi.org/10.1021/acs.iecr.8b00332>

665 Gu, Y., Chen, X., Liu, Z., Zhou, X., Zhang, Y., 2020. Effect of inoculum sources on the anaerobic
666 digestion of rice straw. *Bioresour. Technol.* 158, 149–155.
667 <https://doi.org/10.1016/j.biortech.2014.02.011>

668 Hai, T., Dhahad, H.A., Kumar, P., Fahad, S., Ibrahim, A., Fahmi, A., Attia, E., Shamseldin, M.A.,
669 Najat, A., 2022. Innovative proposal of energy scheme based on biogas from digester for
670 producing clean and sustainable electricity , cooling and heating : Proposal and multi-criteria
671 optimization. *Sustain. Energy Technol. Assessments* 53, 102618.
672 <https://doi.org/10.1016/j.seta.2022.102618>

673 Harun, N., Othman, N.A., Zaki, N.A., Mat Rasul, N.A., Samah, R.A., Hashim, H., 2019. Simulation
674 of Anaerobic Digestion for Biogas Production from Food Waste Using SuperPro Designer.
675 *Mater. Today Proc.* 19, 1315–1320. <https://doi.org/10.1016/j.matpr.2019.11.143>

676 Hendriks, A.T.W.M., Zeeman, G., 2009. Pretreatments to enhance the digestibility of
677 lignocellulosic biomass. *Bioresour. Technol.* 100, 10–18.
678 <https://doi.org/10.1016/j.biortech.2008.05.027>

679 Huang, Y., Ma, Y., Wan, J., Wang, Y., 2021. Modeling the Performance of Full-Scale Anaerobic
680 Biochemical System Treating Deinking Pulp Wastewater Based on Modified Anaerobic
681 Digestion Model No . 1 12, 1–12. <https://doi.org/10.3389/fmicb.2021.755398>

682 Jain, Siddharth, Jain, Shivani, Wolf, I.T., Lee, J., Tong, Y.W., 2015. A comprehensive review on
683 operating parameters and different pretreatment methodologies for anaerobic digestion of
684 municipal solid waste. *Renew. Sustain. Energy Rev.* 52, 142–154.
685 <https://doi.org/10.1016/j.rser.2015.07.091>

686 Kainthola, J., Kalamdhad, A.S., Goud, V. V., 2019. A review on enhanced biogas production from
687 anaerobic digestion of lignocellulosic biomass by different enhancement techniques. *Process*
688 *Biochem.* 84, 81–90. <https://doi.org/10.1016/j.procbio.2019.05.023>

689 Karthikeyan, O.P., Trably, E., Mehariya, S., Bernet, N., Wong, J.W.C., Carrere, H., 2018.
690 Pretreatment of food waste for methane and hydrogen recovery : A review. *Bioresour.*
691 *Technol.* 249, 1025–1039. <https://doi.org/10.1016/j.biortech.2017.09.105>

692 Kawai, M., Nagao, N., Tajima, N., Niwa, C., Matsuyama, T., Toda, T., 2014. The effect of the
693 labile organic fraction in food waste and the substrate / inoculum ratio on anaerobic digestion
694 for a reliable methane yield. *Bioresour. Technol.* 157, 174–180.
695 <https://doi.org/10.1016/j.biortech.2014.01.018>

696 Kianmehr, P., Parker, W., Seto, P., 2010. An evaluation of protocols for characterization of ozone
697 impacts on WAS properties and digestibility. *Bioresour. Technol.* 101, 8565–8572.
698 <https://doi.org/10.1016/j.biortech.2010.06.061>

699 Kovalovszki, A., Treu, L., Ellegaard, L., Luo, G., Angelidaki, I., 2020. Modeling temperature
700 response in bioenergy production : Novel solution to a common challenge of anaerobic
701 digestion. *Appl. Energy* 263, 114646. <https://doi.org/10.1016/j.apenergy.2020.114646>

702 Kumar Biswal, B., Huang, H., Dai, J., Chen, G.H., Wu, D., 2020. Impact of low-thermal
703 pretreatment on physicochemical properties of saline waste activated sludge, hydrolysis of
704 organics and methane yield in anaerobic digestion. *Bioresour. Technol.* 297.

705 <https://doi.org/10.1016/j.biortech.2019.122423>

706 Lauberte, L., Telysheva, G., Cravotto, G., Andersone, A., Janceva, S., Dizhbite, T., Arshanitsa, A.,
707 Jurkjane, V., Vevere, L., Grillo, G., Calcio, E., Tabasso, S., 2021. Lignin e Derived
708 antioxidants as value-added products obtained under cavitation treatments of the wheat straw
709 processing for sugar production. *J. Clean. Prod.* 303, 126369.
710 <https://doi.org/10.1016/j.jclepro.2021.126369>

711 Li, L., He, Q., Zhao, X., Wu, D., Wang, X., Peng, X., 2018. Anaerobic digestion of food waste:
712 Correlation of kinetic parameters with operational conditions and process performance.
713 *Biochem. Eng. J.* 130, 1–9. <https://doi.org/10.1016/j.bej.2017.11.003>

714 Li, Y., Chen, Y., Wu, J., 2019. Enhancement of methane production in anaerobic digestion process:
715 A review. *Appl. Energy* 240, 120–137. <https://doi.org/10.1016/j.apenergy.2019.01.243>

716 Li, Y., Jin, Y., Li, J., Li, H., Yu, Z., Nie, Y., 2017. Effects of thermal pretreatment on degradation
717 kinetics of organics during kitchen waste anaerobic digestion. *Energy* 118, 377–386.
718 <https://doi.org/10.1016/j.energy.2016.12.041>

719 Liu, Y., Fang, J., Tong, X., Huan, C., Ji, G., Zeng, Y., 2019. Change to biogas production in solid-
720 state anaerobic digestion using rice straw as substrates at different temperatures. *Bioresour.*
721 *Technol.* 293, 122066. <https://doi.org/10.1016/j.biortech.2019.122066>

722 Mancini, E., Raggi, A., 2021. A review of circularity and sustainability in anaerobic digestion
723 processes. *J. Environ. Manage.* 291, 112695. <https://doi.org/10.1016/j.jenvman.2021.112695>

724 Mehr, A.S., Gandiglio, M., Mosayebnezhad, M., Lanzini, A., Mahmoudi, S.M.S., Yari, M.,
725 Santarelli, M., 2017. Solar-assisted integrated biogas solid oxide fuel cell (SOFC) installation
726 in wastewater treatment plant : Energy and economic analysis. *Appl. Energy* 191, 620–638.
727 <https://doi.org/10.1016/j.apenergy.2017.01.070>

728 Menardo, S., Cacciatore, V., Balsari, P., 2015. Batch and continuous biogas production arising from
729 feed varying in rice straw volumes following pre-treatment with extrusion. *Bioresour. Technol.*
730 180, 154–161. <https://doi.org/10.1016/j.biortech.2014.12.104>

731 Motte, J.C., Escudíé, R., Hamelin, J., Steyer, J.P., Bernet, N., Delgenes, J.P., Dumas, C., 2015.
732 Substrate milling pretreatment as a key parameter for Solid-State Anaerobic Digestion
733 optimization. *Bioresour. Technol.* 173, 185–192.
734 <https://doi.org/10.1016/j.biortech.2014.09.015>

735 Naran, E., Toor, U.A., Kim, D.J., 2016. Effect of pretreatment and anaerobic co-digestion of food
736 waste and waste activated sludge on stabilization and methane production. *Int. Biodeterior.*
737 *Biodegrad.* 113, 17–21. <https://doi.org/10.1016/j.ibiod.2016.04.011>

738 Panigrahi, S., Sharma, H.B., Dubey, B.K., 2020. Anaerobic co-digestion of food waste with
739 pretreated yard waste: A comparative study of methane production, kinetic modeling and
740 energy balance. *J. Clean. Prod.* 243, 118480. <https://doi.org/10.1016/j.jclepro.2019.118480>

741 Pilli, S., Bhunia, P., Yan, S., LeBlanc, R.J., Tyagi, R.D., Surampalli, R.Y., 2011. Ultrasonic
742 pretreatment of sludge: A review. *Ultrason. Sonochem.* 18, 1–18.
743 <https://doi.org/10.1016/j.ultsonch.2010.02.014>

744 Pleissner, D., Peinemann, J.C., 2020. The Challenges of Using Organic Municipal Solid Waste as
745 Source of Secondary Raw Materials. *Waste Biomass Valorization* 11, 435–446.
746 <https://doi.org/10.1007/s12649-018-0497-1>

747 Rajput, A.A., Zeshan, Visvanathan, C., 2018. Effect of thermal pretreatment on chemical
748 composition, physical structure and biogas production kinetics of wheat straw. *J. Environ.*
749 *Manage.* 221, 45–52. <https://doi.org/10.1016/j.jenvman.2018.05.011>

750 Rasapoor, M., Ajabshirchi, Y., Adl, M., Abdi, R., Gharibi, A., 2016. The effect of ultrasonic
751 pretreatment on biogas generation yield from organic fraction of municipal solid waste under
752 medium solids concentration circumstance. *Energy Convers. Manag.* 119, 444–452.
753 <https://doi.org/10.1016/j.enconman.2016.04.066>

754 Rillo, E., Gandiglio, M., Lanzini, A., Bobba, S., Santarelli, M., Blengini, G., 2020. Life Cycle
755 Assessment (LCA) of biogas-fed Solid Oxide Fuel Cell (SOFC) plant. *Energy* 126, 585–
756 602. <https://doi.org/10.1016/j.energy.2017.03.041>

757 Rittmann, S.K.M.R., Seifert, A.H., Bernacchi, S., 2018. Kinetics, multivariate statistical modelling,
758 and physiology of CO₂-based biological methane production. *Appl. Energy* 216, 751–760.
759 <https://doi.org/10.1016/j.apenergy.2018.01.075>

760 Saxena, S., Saharan, V.K., George, S., 2019. Modeling & simulation studies on batch anaerobic
761 digestion of hydrodynamically cavitated tannery waste effluent for higher biogas yield.
762 *Ultrason. Sonochem.* 58, 104692. <https://doi.org/10.1016/j.ultsonch.2019.104692>

763 Scherzinger, M., Kaltschmitt, M., 2021. Thermal pre-treatment options to enhance anaerobic
764 digestibility – A review. *Renew. Sustain. Energy Rev.* 137, 110627.
765 <https://doi.org/10.1016/j.rser.2020.110627>

766 Suksong, W., Mamimin, C., Prasertsan, P., Kongjan, P., 2019. Effect of inoculum types and
767 microbial community on thermophilic and mesophilic solid-state anaerobic digestion of empty
768 fruit bunches for biogas production. *Ind. Crop. Prod.* 133, 193–202.
769 <https://doi.org/10.1016/j.indcrop.2019.03.005>

770 Victorin, M., Davidsson, Å., Wallberg, O., 2020. Characterization of Mechanically Pretreated
771 Wheat Straw for Biogas Production. *Bioenergy Res.* 13, 833–844.
772 <https://doi.org/10.1007/s12155-020-10126-7>

773 Wang, L., Long, F., Liao, W., Liu, H., 2020. Prediction of anaerobic digestion performance and
774 identification of critical operational parameters using machine learning algorithms. *Bioresour.*
775 *Technol.* 298, 122495. <https://doi.org/10.1016/j.biortech.2019.122495>

776 Zhang, J, Luo, W., Wang, Y., Li, G., Liu, Y., Gong, X., 2019a. Anaerobic cultivation of waste
777 activated sludge to inoculate solid state anaerobic co-digestion of agricultural wastes : Effects
778 of different cultivated periods. *Bioresour. Technol.* 294, 122078.
779 <https://doi.org/10.1016/j.biortech.2019.122078>

780 Zhang, J, Mao, L., Nithya, K., Loh, K.C., Dai, Y., He, Y., Wah Tong, Y., 2019b. Optimizing
781 mixing strategy to improve the performance of an anaerobic digestion waste-to-energy system
782 for energy recovery from food waste. *Appl. Energy* 249, 28–36.

783 <https://doi.org/10.1016/j.apenergy.2019.04.142>

784 Zhang, L., Loh, K.C., Zhang, J., 2019. Enhanced biogas production from anaerobic digestion of
785 solid organic wastes: Current status and prospects. *Bioresour. Technol. Reports* 5, 280–296.
786 <https://doi.org/10.1016/j.biteb.2018.07.005>

787 Zhang, Y., Banks, C.J., 2013. Impact of different particle size distributions on anaerobic digestion
788 of the organic fraction of municipal solid waste. *Waste Manag.* 33, 297–307.
789 <https://doi.org/10.1016/j.wasman.2012.09.024>

790 Zhen, G., Lu, X., Kato, H., Zhao, Y., Li, Y.Y., 2017. Overview of pretreatment strategies for
791 enhancing sewage sludge disintegration and subsequent anaerobic digestion: Current advances,
792 full-scale application and future perspectives. *Renew. Sustain. Energy Rev.* 69, 559–577.
793 <https://doi.org/10.1016/j.rser.2016.11.187>

794